Inorganic Chemistry
Article

Inorg. Chem. **2009**, *48*, 7937–7946 **7937**
DOI: 10.1021/ic900888m

Surprisingly Bright Near-Infrared Luminescence and Short Radiative Lifetimes of Ytterbium in Hetero-Binuclear Yb−Na Chelates

Nail M. Shavaleev, Rosario Scopelliti, Frédéric Gumy, and Jean-Claude G. Bünzli*

École Polytechnique Fédérale de Lausanne, Laboratory of Lanthanide Supramolecular Chemistry, BCH 1405, CH-1015 Lausanne, Switzerland

Received May 7, 2009

New heterobinuclear lanthanide complexes with benzoxazole-substituted 8-hydroxyquinolines, $[Ln(ligand)_2(\mu\text{-ligand})_2Na]$ (Ln: Yb, Lu), have been prepared and their structure established by X-ray crystallography, ^1H NMR spectroscopy, and photophysical studies. The complexes display efficient ligand-sensitized near-infrared luminescence of ytterbium at 925−1075 nm with lifetimes and quantum yields as high as 22 μs and 3.7%, in the solid state, and 20 μs and 2.6% in CH_2Cl_2 solution, respectively. These quantum yields are the highest reported to date for ytterbium complexes with organic ligands containing C−H bonds. A long-wavelength and intense intraligand charge-transfer transition (λ_{max} = 446−456 nm; $\varepsilon \approx 1.2\times10^4\ M^{-1}\ cm^{-1}$) allows for the excitation of infrared luminescence with visible light up to 600 nm. Remarkable features of these complexes include (i) quantitative ligand-to-Yb^{III} energy transfer resulting in high overall efficiency of the ytterbium luminescence, (ii) unusually short radiative lifetime of the Yb^{III} ion, 706−745 μs for solutions in CH_2Cl_2, calculated from the f−f absorption spectra, and 513−635 μs estimated for solid state samples from quantum yield and lifetime data, and (iii) the unexpected large influence of second-sphere composition on the radiative lifetime of ytterbium.

Introduction

The trivalent ytterbium ion is one of the most efficient near-infrared (NIR) emitters among lanthanides,[1] a result of the relatively large energy gap,[2] 10 250 cm^{-1}, between its emitting level and the ground state. The luminescence quantum yields for anhydrous organic complexes of Yb^{III} containing C−H bonds are reported to be in the range 0.6−2.1%[3−10] and are substantially increased upon perdeuteration[11,12] or perfluorination[13,14] of the ligands. With respect to applications, ytterbium chelates are important as emitters in NIR electroluminescence devices[15−17] and sensors in biomedical analyses, imaging, and therapy: for instance, its porphyrin complexes have been tested in the photodynamic therapy of cancer and NIR luminescence localization of tumors,[18,19] and Yb^{III} emission has been recorded in the presence of proteins[20,21] and nucleic acids.[22,23] However, attempts to

*To whom correspondence should be addressed. E-mail: jean-claude.bunzli@epfl.ch.

(1) Comby, S.; Bünzli, J.-C. G. Lanthanide Near-Infrared Luminescence in Molecular Probes and Devices. In *Handbook on the Physics and Chemistry of Rare Earths*; Gschneidner, K. A., Jr., Bünzli, J.-C. G., Pecharsky, V. K., Eds.; Elsevier Science B.V.: Amsterdam, 2007; Vol. *37*, Chapter 235, pp 217−470.
(2) Carnall, W. T. The Absorption and Fluorescence Spectra of Rare Earth Ions in Solution. In *Handbook on the Physics and Chemistry of Rare Earths*; Gschneidner, K. A., Jr., Eyring, L., Eds.; North Holland Publishing Co.: Amsterdam, 1979; Vol. *3*, Chapter 24, pp 172−208.
(3) Venchikov, V. Ya.; Tsvirko, M. P. *J. Appl. Spectrosc.* **2000**, *67*, 745.
(4) Tsvirko, M. P.; Meshkova, S. B.; Venchikov, V. Ya.; Topilova, Z. M.; Bol'shoi, D. V. *Opt. Spectrosc.* **2001**, *90*, 669.
(5) Rusakova, N. V.; Korovin, V. Y.; Zhilina, Z. I.; Vodzinskii, S. V.; Ishkov, Yu. V. *J. Appl. Spectrosc.* **2004**, *71*, 506.
(6) Albrecht, M.; Osetska, O.; Klankermayer, J.; Fröhlich, R.; Gumy, F.; Bünzli, J.-C. G. *Chem. Commun.* **2007**, 1834.
(7) Albrecht, M.; Osetska, O.; Fröhlich, R.; Bünzli, J.-C. G.; Aebischer, A.; Gumy, F.; Hamacek, J. *J. Am. Chem. Soc.* **2007**, *129*, 14178.
(8) Jiang, F. L.; Wong, W. K.; Zhu, X. J.; Zhou, G. J.; Wong, W. Y.; Wu, P. L.; Tam, H. L.; Cheah, K. W.; Ye, C.; Liu, Y. *Eur. J. Inorg. Chem.* **2007**, 3365.
(9) He, H.; Sykes, A. G. *Inorg. Chem. Commun.* **2008**, *11*, 1304.
(10) Huang, W.; Wu, D.; Guo, D.; Zhu, X.; He, C.; Meng, Q.; Duan, C. *Dalton Trans.* **2009**, 2081.
(11) Tsvirko, M. P.; Kachura, T. F. *J. Appl. Spectrosc.* **1975**, *23*, 1527.
(12) Hebbink, G. A.; Reinhoudt, D. N.; Van Veggel, F. C. J. M. *Eur. J. Org. Chem.* **2001**, 4101.
(13) Glover, P. B.; Bassett, A. P.; Nockemann, P.; Kariuki, B. M.; Van Deun, R.; Pikramenou, Z. *Chem.—Eur. J.* **2007**, *13*, 6308.
(14) Hasegawa, Y.; Yasuda, T.; Nakamura, K.; Kawai, T. *Jpn. J. Appl. Phys.* **2008**, *47*, 1192.
(15) Kawamura, Y.; Wada, Y.; Iwamuro, M.; Kitamura, T.; Yanagida, S. *Chem. Lett.* **2000**, 280.
(16) Hong, Z. R.; Liang, C. J.; Li, R. G.; Zhao, D.; Fan, D.; Li, W. L. *Thin Solid Films* **2001**, *391*, 122.
(17) Khreis, O. M.; Gillin, W. P.; Somerton, M.; Curry, R. J. *Org. Electron.* **2001**, *2*, 45.
(18) Gaiduk, M. I.; Grigoryants, V. V.; Mironov, A. F.; Rumyantseva, V. D.; Chissov, V. I.; Sukhin, G. M. *J. Photochem. Photobiol. B: Biol.* **1990**, *7*, 15.
(19) Jiang, F. L.; Poon, C. T.; Wong, W. K.; Koon, H. K.; Mak, N. K.; Choi, C. Y.; Kwong, D. W. J.; Liu, Y. *ChemBioChem* **2008**, *9*, 1034.
(20) Horrocks, W. DeW., Jr.; Bolender, J. P.; Smith, W. D.; Supkowski, R. M. *J. Am. Chem. Soc.* **1997**, *119*, 5972.
(21) Chudinov, A. V.; Rumyantseva, V. D.; Lobanov, A. V.; Chudinova, G. K.; Stomakhin, A. A.; Mironov, A. F. *Russ. J. Bioorg. Chem.* **2004**, *30*, 89.
(22) Beeby, A.; Dickins, R. S.; FitzGerald, S.; Govenlock, L. J.; Parker, D.; Williams, J. A. G.; Maupin, C. L.; Riehl, J. P.; Siligardi, G. *Chem. Commun.* **2000**, 1183.
(23) Nonat, A. M.; Quinn, S. J.; Gunnlaugsson, T. *Inorg. Chem.* **2009**, *48*, 4646.

Published on Web 06/25/2009

Scheme 1. Synthesis and Structures of Ligands and Complexes[a]

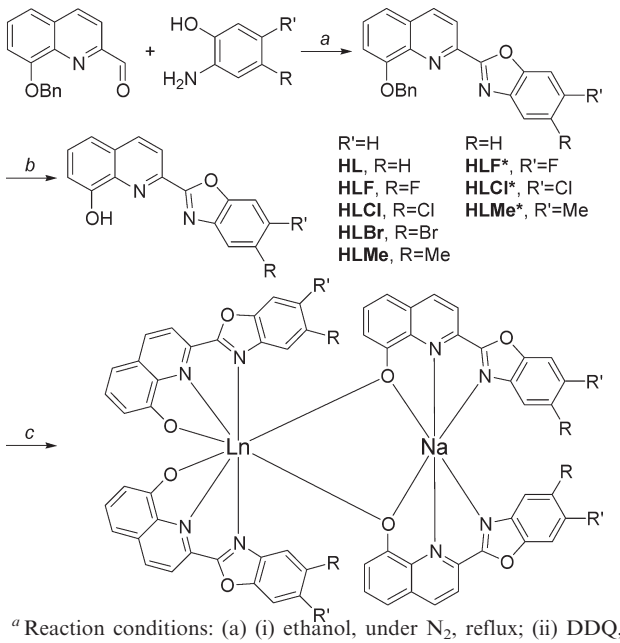

[a] Reaction conditions: (a) (i) ethanol, under N_2, reflux; (ii) DDQ, CH_2Cl_2, under N_2, RT to 40 °C; (b) BBr_3, CH_2Cl_2, under N_2, RT; (c) THF/water, $LnCl_3 \cdot 6H_2O$ (Ln: Yb, Lu), NaOH, under air, heating.

develop practical luminescent bioanalytical labels based on Yb^{III} are hampered by the low quantum yields exhibited by its organic complexes in aqueous solutions, which remain below 0.5%.[24−28]

Ytterbium is a special lanthanide ion with respect to the sensitization of its luminescence in that several mechanisms can be implied,[1] for example, phonon-assisted energy transfer from the triplet state of the ligand,[29,30] or excitation through a reversible ligand-to-Yb^{III} charge-transfer state.[20] However, the low quantum yields of ytterbium complexes reported in the literature are independent of the excitation mechanisms and essentially arise from efficient deactivation by high-energy vibrations of the X−H (X = O, N, C) bonds in the ligands.[1] This major problem is difficult to overcome since it requires designing a rigid metal-ion environment devoid of X−H groups.[11−14]

Recently, we have described NIR-luminescent mononuclear lanthanide complexes with benzoxazole-substituted 8-hydroxyquinolines.[31] In the course of our studies, we have noticed that these ligands react with Yb^{III} ions in the presence of Na^{I} to form binuclear $Yb^{III}-Na^{I}$ chelates, which are unusual in terms of their structure (Scheme 1) and photophysical properties. In this report, we describe the synthesis and characterization of these complexes and discuss the influence of the substitution at the benzoxazole ring on their photophysical data. We also devote attention to estimating the radiative lifetime of the lanthanide ion, which is an essential (but often neglected) parameter in the analysis of photophysical properties and in the calculation of the ligand efficiency for sensitization of lanthanide luminescence.

Results and Discussion

Synthesis. The ligands have been prepared following the previously reported general synthesis[31] of benzoxazole-substituted 8-hydroxyquinolines (Scheme 1). Five ligands are new, while HL,[31,32] HLCl,[31] and HLBr[31] have already been described. The lanthanide complexes $[Ln(ligand)_2(\mu\text{-ligand})_2Na] \cdot nH_2O$ ($n = 0-1$; Ln = Yb, Lu), hereafter denoted as $Na[Ln(ligand)_4] \cdot nH_2O$, have been obtained as air- and moisture-stable orange or dark red solids from THF/water solutions starting with a stoichiometric 4:4:1 molar ratio of the ligand, NaOH, and $LnCl_3 \cdot 6H_2O$. They have been identified by C, H, N elemental analysis; X-ray crystallography; and ^1H NMR spectroscopy.

X-Ray Structural Studies. The crystal and molecular structures of five ytterbium complexes are shown in Figure 1, while selected parameters are collected in Tables 1 and S1 (Supporting Information).

All of the complexes share similar structural properties. The Yb^{III} ion is eight-coordinate by two terminal tridentate ligands and by two bridging ligands bound only via the phenolate oxygen. The ligands are nearly planar, the dihedral angles between quinoline and benzoxazole groups being slightly larger for the bridging ligands (8.9−12.5°) compared to the terminal ones (3.5−9.1°). The terminal ligands are mutually orthogonal with dihedral angles of 82−90° (the planes are defined by the C, N, and O atoms of the core rings and phenolate O atom); the same applies to the bridging ligands, for which angles are 86−87° (the LF^{*-} complex is an exception, 66.3°). Within a complex, $\pi-\pi$ interaction is likely taking place between the terminal and bridging ligands. Although their aromatic rings do not completely overlap and are not always parallel, the distances between them can be as short as 3.5 Å.

The ligands are arranged in an "up−up−up−up" fashion around Yb^{III}. The coordination environment can be described as a distorted trigonal dodecahedron of D_{2d} symmetry with pairs of N atoms from the terminal ligands spanning *a* edges.[33] The N, N, and O atoms of a terminal ligand and the μ-O atom of a bridging ligand are coplanar; two such planes, shown in Figure 2, are orthogonal, the angle being 88−90°. The cores of the complexes feature a nearly planar $Na(\mu\text{-O})_2Yb$ square with a Na−Yb distance of ≈ 3.5 Å; the "folding" of the square, defined as the angle between the $(\mu\text{-O})_2Yb$ and $(\mu\text{-O})_2Na$ planes, is < 12°. The pairs of bridging and terminal ligands are roughly related to each other by a "screw" angle of 35−41° between the $(O)_2Yb$ and $(\mu\text{-O})_2Yb$ planes. The complexes have an approximate overall C_2 symmetry with the corresponding axis passing through the Na and Yb atoms.

(24) Ala-Kleme, T.; Haapakka, K.; Latva, M. *Anal. Chim. Acta* **1999**, *395*, 205.
(25) Comby, S.; Imbert, D.; Vandevyver, C. D. B.; Bünzli, J.-C. G. *Chem.—Eur. J.* **2007**, *13*, 936.
(26) Comby, S.; Imbert, D.; Chauvin, A. S.; Bünzli, J.-C. G. *Inorg. Chem.* **2006**, *45*, 732.
(27) Mato-Iglesias, M.; Rodriguez-Blas, T.; Platas-Iglesias, C.; Starck, M.; Kadjane, P.; Ziessel, R.; Charbonnière, L. *Inorg. Chem.* **2009**, *48*, 1507.
(28) Nonat, A.; Imbert, D.; Pécaut, J.; Giraud, M.; Mazzanti, M. *Inorg. Chem.* **2009**, *48*, 4207.
(29) Crosby, G. A.; Kasha, M. *Spectrochim. Acta* **1958**, *10*, 377.
(30) Reinhard, C.; Güdel, H. U. *Inorg. Chem.* **2002**, *41*, 1048.
(31) Shavaleev, N. M.; Scopelliti, R.; Gumy, F.; Bünzli, J.-C. G. *Inorg. Chem.* **2009**, *48*, 2908.
(32) Kim, J. S.; Choi, M. G.; Huh, Y.; Kim, M. H.; Kim, S. H.; Wang, S. Y.; Chang, S.-K. *Bull. Korean Chem. Soc.* **2006**, *27*, 2058.
(33) Thompson, L. C. Complexes. In *Handbook on the Physics and Chemistry of Rare Earths*; Gschneidner, K. A., Jr., Eyring, L., Eds.; North Holland Publishing Co.: Amsterdam, 1979; Vol. *3*, Chapter 25, pp 209−297.

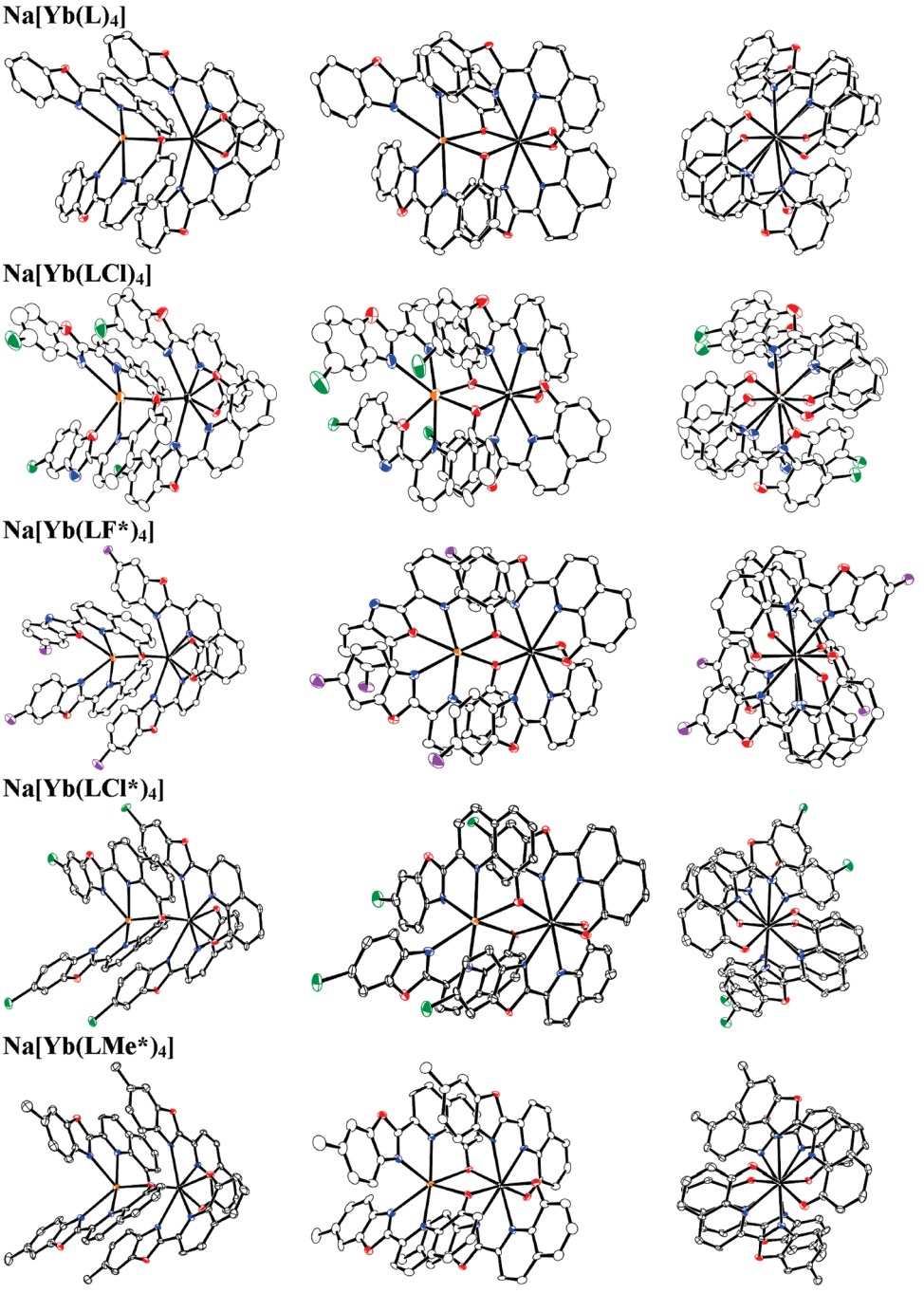

Figure 1. Molecular structures of the complexes Na[Yb(ligand)$_4$] (three views, 50% probability ellipsoids, H atoms and cocrystallized solvent molecules omitted). Heteroatoms: O, red; N, blue; F, purple; Cl, green; Yb, black; Na, orange. The idealized C_2 axis runs through Na and Yb and is in the plane of the paper (left, middle) or perpendicular to it (right).

The ligands are not equally strongly bonded to the metal ion, as reflected in the different sets of bond lengths within pairs of bridging and terminal ligands. The Yb^{III} ion is preferentially bound to the 8-hydroxyquinoline, while bonding to the N atom of benzoxazole is weaker, resulting in longer bond lengths and wider range variation: Yb−O, 2.229−2.281 Å (Δ = 0.052 Å); Yb−μ-O, 2.238−2.291 Å (Δ = 0.053 Å); Yb−N(q), 2.453−2.486 Å (Δ = 0.033 Å); Yb−N(b), 2.565−2.662 (Δ = 0.097 Å). The Yb−O and Yb−μ-O distances are similar, and metal−ligand bond lengths do not depend significantly on the presence of an electron-withdrawing (F, Cl) or -donating (CH_3) group in the positions 5 or 6 of the benzoxazole ring.

The relative bonding strength of the ligands has been quantified using the bond-valence method,[34] wherein a donor atom j lying at a distance $d_{Ln,j}$ from the metal ion is characterized by a bond-valence contribution $\nu_{Ln,j}$:

$$\nu_{Ln,j} = e^{(R_{Ln,j} - d_{Ln,j})/b} \quad (1)$$

where $R_{Ln,j}$ represents the bond-valence parameters depending on the pair of interacting atoms (Yb−O[35]

(34) Brown, I. D.; Altermatt, D. *Acta Crystallogr., Sect. B* **1985**, *41*, 244.
(35) Trzesowska, A.; Kruszynski, R.; Bartczak, T. J. *Acta Crystallogr., Sect. B* **2004**, *60*, 174.

Table 1. Selected Structural Parameters of the Complexes[a]

	bond lengths (Å)[b]				angles (deg)					
complex	Ln−μ-O	Ln−O	Ln−N(q)	Ln−N(b)	q−b[c]	μ-q−b[c]	α[d]	β[e]	Yb−Na (Å)[f]	Yb−Yb (Å)[f]
Na[Yb(L)$_4$]		2.262(4)	2.464(5)	2.600(5)	7.20		4.67	35.29	3.5403(14)	9.304
		2.269(4)	2.474(5)	2.662(6)	10.99					
	2.238(4)					12.60				
	2.250(4)					12.36				
	2.244	**2.266**	**2.469**	**2.631**	**9.10**	**12.48**				
Na[Yb(LCl)$_4$]		2.229(10)	2.466(12)	2.607(12)	6.60		7.69	34.97	3.485(6)	8.969
		2.264(10)	2.486(6)	2.634(12)	9.94					
	2.248(10)					11.06				
	2.254(10)					6.78				
	2.251	**2.247**	**2.476**	**2.621**	**8.27**	**8.92**				
Na[Yb(LF*)$_4$]		2.250(5)	2.473(4)	2.622(4)	4.72		6.77	41.15	3.4357(19)	9.360
		2.281(5)	2.482(4)	2.629(4)	2.28					
	2.251(3)					11.01				
	2.291(3)					12.00				
	2.271	**2.266**	**2.478**	**2.626**	**3.50**	**11.51**				
Na[Yb(LCl*)$_4$]		2.256(6)	2.463(7)	2.566(7)	5.10		11.86	37.05	3.550(4)	9.080
		2.272(6)	2.478(7)	2.604(8)	3.72					
	2.251(6)					11.49				
	2.263(6)					7.09				
	2.257	**2.264**	**2.471**	**2.585**	**4.41**	**9.29**				
Na[Yb(LMe*)$_4$]		2.251(5)	2.453(6)	2.565(5)	3.54		10.23	37.69	3.556(3)	9.227
		2.280(5)	2.470(6)	2.590(6)	5.86					
	2.263(5)					10.34				
	2.263(5)					9.95				
	2.263	**2.266**	**2.462**	**2.578**	**4.70**	**10.15**				

[a] Each line in the table corresponds to one and the same ligand in the complex (whenever appropriate). Numbers in bold are averaged data. [b] N(q) and N(b) are nitrogen atoms of quinoline and benzoxazole, respectively. [c] Dihedral angles between the planes of quinoline and benzoxazole (defined by the C, N, and O atoms of the core rings) in the terminal (q−b) and bridging (μ-q−b) ligands. [d] "Folding" of the Na(μ-O)$_2$Yb square defined by the dihedral angle between the (μ-O)$_2$Yb and (μ-O)$_2$Na planes. [e] Dihedral "screw" angle between the (O)$_2$Yb and (μ-O)$_2$Yb planes. [f] The shortest Yb−Na and Yb−Yb distances in the structure.

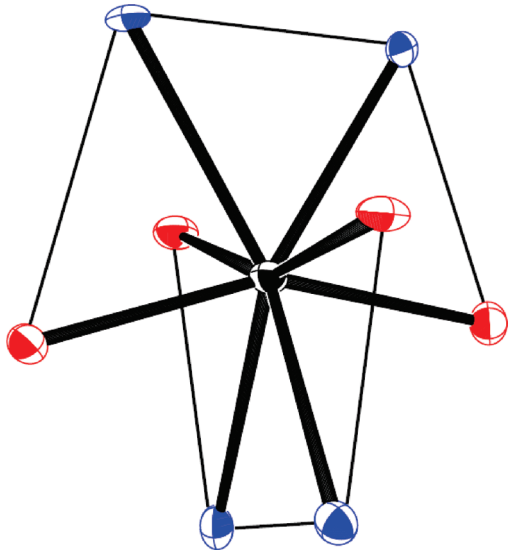

Figure 2. Coordination environment of Yb^{III} in Na[Yb(L)$_4$], representative of all discussed complexes. Heteroatoms: O, red; N, blue; Yb, black. The atoms connected by a line are coplanar.

or Yb−N[36]) and b is a constant equal to 0.37 Å.[34] The bond valence sum (BVS) of the metal ion V_{Ln} defined by eq 2 is supposed to match its formal oxidation state if average bond distances are standard:[34]

$$V_{Ln} = \sum_j \nu_{Ln,j} \qquad (2)$$

The BVSs for the new structures are in the range of 2.88−2.91, with the exception of Na[Yb(LF*)$_4$], which has a smaller BVS of 2.81. The average BVS amounts to 2.88(4) (Table 2), slightly less than expected for Yb^{III} (3.00) but within the variability of the method, accepted to be ±0.25 valence units. This confirms the good quality of the crystallographic data and probably reflects the somewhat elongated Yb−N(b) bonds (see above). The smaller BVS for Na[Yb(LF*)$_4$] with respect to LCl*$^-$ and LMe*$^-$ complexes is mainly due to a smaller contribution from the Yb−N(b) bonds. The average contributions from the various coordinating groups are nearly constant and are in the expected order: ν(O) = 0.43(2) ≈ ν(μ-O) = 0.44(2) > ν(N-py) = 0.33(1) > ν(N-b) = 0.23(2).

With respect to potential intermolecular interactions, the Yb−Yb distances are >8.969 Å so that energy migration between metal centers is likely to be prevented. The cocrystallized water molecule in Na[Yb(LF*)$_4$]·H_2O·CH_2Cl_2 is hydrogen-bonded to a phenolate oxygen of one of the terminal ligands with a O···O distance of 2.919(8) Å, while the distance Yb···O(water) is 4.514 Å. This is the only complex for which X-ray analysis demonstrated the presence of a water molecule.

Finally, the sodium cation is six-coordinate by the two bridging ligands. The benzoxazole ring is bound to sodium via the N atom in the L$^-$, LCl*$^-$, and LMe*$^-$ complexes. In Na[Yb(LF*)$_4$], one benzoxazole is coordinated with the O atom and the other with the N atom. Finally, in Na[Yb(LCl)$_4$], one benzoxazole binds with its O atom, while the other is disordered and binds either with the O or N atom. Overall, sodium−ligand bond lengths sustain large variations: Na−N(q), 2.319−2.473

(36) Trzesowska, A.; Kruszynski, R.; Bartczak, T. J. *Acta Crystallogr., Sect. B* **2005**, *61*, 429.

Table 2. Calculated Bond Valence Parameters

		$v_{Yb,f}$(O)			$v_{Yb,f}$(N)		
complex	V_{Yb}	O	μ-O	O(av.)	N(q)[a]	N(b)[a]	N(av.)
Na[Yb(L)$_4$]	2.88	0.43(1)	0.46(1)	0.44(2)	0.33(1)	0.22(3)	0.28(7)
Na[Yb(LCl)$_4$]	2.91	0.45(3)	0.45(1)	0.45(2)	0.33(1)	0.22(1)	0.28(6)
Na[Yb(LF*)$_4$]	2.81	0.43(3)	0.43(3)	0.43(2)	0.33(1)	0.22(1)	0.27(6)
Na[Yb(LCl*)$_4$]	2.90	0.43(1)	0.44(1)	0.44(1)	0.33(1)	0.24(2)	0.29(5)
Na[Yb(LMe*)$_4$]	2.91	0.43(2)	0.43(0)	0.43(1)	0.34(1)	0.25(1)	0.30(5)
all data	2.88(4)	0.43(2)	0.44(2)	0.44(2)	0.33(1)	0.23(2)	0.28(5)

[a] N(q) and N(b) are nitrogen atoms of quinoline and benzoxazole, respectively.

Å ($\Delta = 0.154$ Å); Na−μ-O, 2.336−2.548 Å ($\Delta = 0.212$ Å); Na−N(b), 2.521−2.817 Å ($\Delta = 0.296$ Å); Na−O(b), 2.599−2.801 Å ($\Delta = 0.202$ Å) (Table S1, Supporting Information).

In conclusion, the heterobinuclear chelates [Ln(ligand)$_2$(μ-ligand)$_2$Na] described here represent a third structural type of lanthanide complexes with benzoxazole-substituted 8-hydroxyquinolines, the other two being mononuclear species, 9-coordinate [Nd(κ^3-ligand)$_3$] and 8-coordinate [Yb(κ^3-ligand)(κ^1-ligand)·H$_2$O].[31] They are a new entry to a rich structural family of lanthanide 8-hydroxyquinolates,[37−41] which already includes examples of homo- and heterobinuclear triple helicates.[7,42]

^{1}H NMR Spectroscopy of Lutetium Complexes. Diamagnetic lutetium complexes with LF*$^-$ and LMe*$^-$ were sufficiently soluble in a noncoordinating solvent, CD_2Cl_2, to record their ^{1}H NMR spectra. The proton resonances were sharp, and the spectra displayed two sets of signals assigned to the terminal and bridging coordinated ligands. For example, in the LMe*$^-$ complex, two singlets of equal intensity for the methyl group are observed at 2.23 and 1.85 ppm (Figure 3). Therefore, ^{1}H NMR experiments confirm that the complexes remain intact and do not undergo intra- or intermolecular ligand exchange in a 10^{-3} M CH_2Cl_2 solution. Their structure is likely to correspond to that found in the solid state (see also the photophysical data below).

Electronic Spectroscopy. UV−vis absorption spectra of the ligands and complexes have been recorded in CH_2Cl_2 solution at room temperature. They are shown in Figures 4 and Figures S13−S20 (Supporting Information), and their main spectral features are summarized in Table 3. The ligands display several bands only in the UV range with an absorption cutoff at 400 nm due to $\pi \rightarrow \pi^*$ transitions within quinoline and benzoxazole chromophores.[31] Upon deprotonation and complex formation, a broad ligand-centered absorption band appears in the visible with a maximum at 446−456 nm, a shoulder at 525 nm, a cutoff at 600 nm, and $\varepsilon = (1.1-1.2)\times10^4$ M^{-1} cm^{-1}. It is assigned to an intraligand charge-transfer transition (ILCT) wherein phenolate and (quinoline + benzoxazole) moieties serve as electron donors and acceptors, respectively. It accounts for the orange or red color of Na^I salts (Figure S17, Supporting Information) and Ln^{III}−Na^I complexes as opposed to the pale yellow color of the ligands. The intensity of the ILCT transition is $(2.8-3.0)\times10^3$ M^{-1} cm^{-1} per ligand, typical of a metal-coordinated 8-hydroxyquinolate chromophore,[43] while its maximum is red-shifted by up to 10 nm upon substitution in the benzoxazole ring in the order Br > Cl > F > (Me, H), suggesting an electronic communication between the two constituent chromophores of the ligand. The component of the ILCT band corresponding to its maximum at 446−456 nm is assigned to the bridging ligand and the shoulder at 525 nm to the terminal ligand; this conclusion is based on the comparison with the spectral data reported for tris complexes of Nd^{III} wherein the terminal ligands display an ILCT band at λ_{max} 508−527 nm.[31] In the UV range, a single intense transition is observed for the complexes with a maximum at 314−319 nm, a cutoff at 400 nm, and $\varepsilon = (1.3-1.5)\times10^5$ M^{-1} cm^{-1}; the maximum is red-shifted by up to 5 nm upon substitution of the benzoxazole with (Me, Br, Cl) > F > H. The ligand-centered transitions do not depend on the position of the substituent in the benzoxazole ring (5 or 6) and are identical for Yb^{III} and Lu^{III} complexes, as would be expected for these ions of similar radii. For ytterbium complexes with LMe*$^-$ and LF*$^-$, the broad (900−1025 nm) and very weak (11−12 M^{-1} cm^{-1}) metal-centered f−f absorption transition[2] in the near-infrared could be measured; it displays a main maximum at 983 nm (Figure S20, Supporting Information).

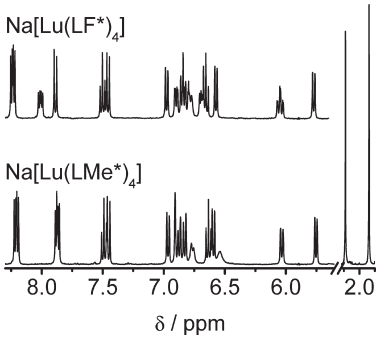

Figure 3. ^{1}H NMR spectra of lutetium complexes in CD_2Cl_2 at room temperature: Na[Lu(LF*)$_4$]·2H$_2$O, 8.81×10^{-4} M; Na[Lu(LMe*)$_4$], 1.00×10^{-3} M.

Near-Infrared Luminescence of Ytterbium. All of the new ytterbium complexes display characteristic metal-centered near-infrared luminescence at 925−1075 nm, with a maximum at ≈985 nm, resulting from the $^2F_{5/2} \rightarrow {}^2F_{7/2}$ transition. Emission is observed both in the solid state and, for the more soluble LF*$^-$ and LMe*$^-$ chelates, in CH_2Cl_2 solution. The corresponding emission spectra are shown in Figure 5 and Figure S21 (Supporting Information),

(37) Van Deun, R.; Fias, P.; Nockemann, P.; Schepers, A.; Parac-Vogt, T. N.; Van Hecke, K.; Van Meervelt, L.; Binnemans, K. *Inorg. Chem.* **2004**, *43*, 8461.
(38) Artizzu, F.; Deplano, P.; Marchio, L.; Mercuri, M. L.; Pilia, L.; Serpe, A.; Quochi, F.; Orru, R.; Cordella, F.; Meinardi, F.; Tubino, R.; Mura, A.; Bongiovanni, G. *Inorg. Chem.* **2005**, *44*, 840.
(39) Katkova, M. A.; Kurskii, Y. A.; Fukin, G. K.; Averyushkin, A. S.; Artamonov, A. N.; Vitukhnovsky, A. G.; Bochkarev, M. N. *Inorg. Chim. Acta* **2005**, *358*, 3625.
(40) Albrecht, M.; Fiege, M.; Osetska, O. *Coord. Chem. Rev.* **2008**, *252*, 812.
(41) Deacon, G. B.; Forsyth, C. M.; Junk, P. C.; Kynast, U.; Meyer, G.; Moore, J.; Sierau, J.; Urbatsch, A. *J. Alloys Compd.* **2008**, *451*, 436.
(42) Shavaleev, N. M.; Scopelliti, R.; Gumy, F.; Bünzli, J.-C. G. *Inorg. Chem.* **2008**, *47*, 9055.
(43) Ballardini, R.; Varani, G.; Indelli, M. T.; Scandola, F. *Inorg. Chem.* **1986**, *25*, 3858.

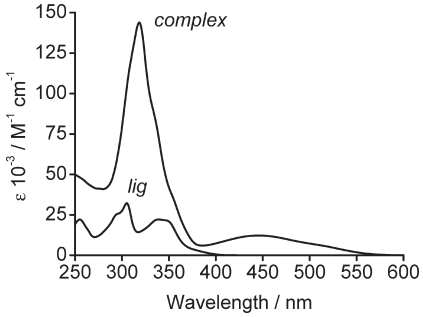

Figure 4. Absorption spectra of ligand HLMe*, 2.39×10^{-4} M, and its complex Na[Yb(LMe*)$_4$], 4.63×10^{-5} M, in CH_2Cl_2. Absorption spectra for the other ligands and complexes are similar and are provided in the Supporting Information.

Table 3. Absorption Spectra of the Ligands and Complexes[a]

compound	λ_{max}/nm (10^{-3} ε/M^{-1} cm^{-1})
HLMe	345 (21), 338 (21), 299 (27), 255 (18)
HLMe*	339 (22), 305 (32), 255 (22)
HLF	343 (19), 331 (18), 297 (28)
HLF*	343 (20), 333 (19), 302 (38), 292 (29), 256 (18)
Na[Yb(L)$_4$]·H_2O	446 (12), 314 (153)
Na[Yb(LF)$_4$]	452 (12), 317 (142)
Na[Yb(LCl)$_4$]·$(H_2O)_{0.5}$	454 (12), 319 (141)
Na[Yb(LBr)$_4$]·$(H_2O)_{0.5}$	456 (12), 319 (141)
Na[Yb(LMe)$_4$]	447 (12), 319 (135)
Na[Lu(LMe)$_4$]	447 (11), 319 (132)
Na[Yb(LF*)$_4$]·H_2O	983 (0.012), 450 (12), 315 (153)
Na[Lu(LF*)$_4$]·$2H_2O$	451 (11), 315 (149)
Na[Yb(LCl*)$_4$]	455 (12), 318 (157)
Na[Yb(LMe*)$_4$]	983 (0.011), 446 (12), 319 (144)
Na[Lu(LMe*)$_4$]	447 (12), 319 (142)

[a] Recorded at 250−800 nm in CH_2Cl_2 solution, $(1.53-2.39)\times10^{-4}$ M for the ligands and $(3.96-5.57)\times10^{-5}$ M or $(8.03-8.40)\times10^{-4}$ M for the complexes, at room temperature. Estimated errors are ±1 nm for λ_{max} and ±5% for ε.

while the photophysical parameters are summarized in Table 4.

Emission spectra of microcrystalline samples and of the solutions are nearly identical in terms of bandwidth and shape. The high-energy component of the emission spectrum observed at 960 nm at room temperature disappears upon cooling to 77 K (Figure 5) and can therefore be assigned as a "hot" band.[44,45] At 77 K, the emission spectrum displays the expected four components corresponding to the ligand-field splitting of the $^2F_{7/2}$ level; these components are additionally split, by a few cm^{-1}, a fact we attribute to defects in the polycrystalline sample. Luminescence decays are single exponential functions in all cases, pointing to the presence of only one emissive ytterbium center. The observed luminescence lifetimes (τ_{obs}) are in a narrow range of 18−22 μs (Table 4), typical of anhydrous Yb^{III} compounds,[1,46] and are the same in the solid state and in solution, the complex with LF*$^-$ being an exception (see below). The similarity between the photophysical properties of the complexes in solution and

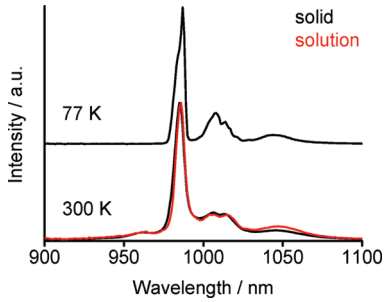

Figure 5. Corrected and normalized luminescence spectra of Na[Yb(LMe*)$_4$] in polycrystalline solid sample and in CH_2Cl_2 solution, 7.71×10^{-4} M, under air, at room temperature and at 77 K. Emission slits are 0.3 nm for the solid sample and 1 nm for the solution. Emission spectra for the other Yb^{III} complexes are similar and are provided in the Supporting Information.

Table 4. Luminescence Properties of Ytterbium Complexes in the Solid State and in 8×10^{-4} M Solutions in CH_2Cl_2 at Room Temperature Under Air

complex		$\tau_{obs}/\mu s$[a]	Q_L^{Yb} /%[b] UV	vis	$\tau_{rad}/\mu s$[c]	Q_{Yb}^{Yb}/%[c]
Na[Yb(L)$_4$]·H_2O	solid	19(1)	3.0	3.1	623	3.0
Na[Yb(LF)$_4$]	solid	20(1)	3.0	3.3	635	3.1
Na[Yb(LCl)$_4$]·$(H_2O)_{0.5}$	solid	19(1)	3.2	3.2	594	3.2
Na[Yb(LBr)$_4$]·$(H_2O)_{0.5}$	solid	18(1)	2.7	3.0	632	2.9
Na[Yb(LMe)$_4$]	solid	22(1)	3.6	3.7	603	3.6
Na[Yb(LF*)$_4$]·H_2O	solid	10(1)	2.0	1.9	513	1.9
Na[Yb(LF*)$_4$]·H_2O	CH_2Cl_2	20(1)		2.4	745[d]	2.7
Na[Yb(LCl*)$_4$]	solid	20(1)	3.6	3.4	571	3.5
Na[Yb(LMe*)$_4$]	solid	22(1)	3.4	3.6	629	3.5
Na[Yb(LMe*)$_4$]	CH_2Cl_2	20(1)		2.6[e]	706[d]	2.8

[a] λ_{exc} = 355 nm for τ; relative error ± 5%. [b] Q_L^{Yb} measured at λ_{exc} 370 nm (UV) and 450 nm (VIS); relative error ± 10%. [c] Calculated from eq 3 assuming η_{sens} = 1 and taking averaged Q_L^{Yb} (UV and VIS); relative error ± 15%. [d] Calculated from eq 4a. [e] Q_L^{Yb} = 3.0% in deaerated CH_2Cl_2.

in the solid state indicates that they remain undissociated in solution.

The presence of an intense ligand-centered ILCT absorption band in the visible for all the complexes allows for convenient excitation of near-infrared luminescence with light up to 600 nm (see the excitation spectrum of Na[Yb(LMe*)$_4$] in Figure S23, Supporting Information). The overall quantum yields of the ligand-sensitized ytterbium luminescence (Q_L^{Yb}) are independent of the excitation wavelength, 370 or 450 nm, within experimental error (Table 4), suggesting that the same mechanism of excitation is operative. The influence of degassing the solution with nitrogen has been checked with Na[Yb(LMe*)]: the quantum yield increases only marginally (< 15%), while the lifetime remains the same. Therefore, assuming that the main path for the energy transfer to Yb^{III} goes through the ligand triplet state, this implies that its rate would be faster than the quenching of the triplet state by oxygen.

The absolute quantum yields are remarkably high, 2.7−3.7% in the solid state (the complex with LF*$^-$ is an exception) and 2.4−2.6% in solution. This is especially unexpected considering that the complexes contain C−H bonds which can potentially quench the excited state of the Yb^{III} ion. Thus, according to the crystal structure analysis, the complexes contain 6, 10, and 23 (21 for LCl$^-$) C−H bonds with intramolecular Yb···H distances less

(44) Asano-Someda, M.; Kaizu, Y. J. *Photochem. Photobiol. A: Chem.* **2001**, *139*, 161.
(45) Goncalves e Silva, F.; Malta, O. L.; Reinhard, C.; Güdel, H. U.; Piguet, C.; Moser, J. E.; Bünzli, J.-C. G. *J. Phys. Chem. A* **2002**, *106*, 1670.
(46) Beeby, A.; Dickins, R. S.; Faulkner, S.; Parker, D.; Williams, J. A. G. *Chem. Commun.* **1997**, 1401.

than 5, 6, and 7 Å, respectively. For instance, the reported quantum yields for ytterbium chelates containing C−H groups do not exceed 2.1%,[3−5,8,9] while for 8-hydroxyquinolates,[6,7,10,25,26,28] they are $< 1.4\%$.[6]

The complex $Na[Yb(LF^*)_4]\cdot H_2O$ is an exception with respect to photophysical properties in the solid state, probably because it contains a cocrystallized water molecule which, according to the X-ray analysis, is hydrogen-bonded to the ligand and is situated at a short distance of 4.514 Å from ytterbium. We suggest that this water quenches the excited state of Yb^{III} via a second-sphere interaction in the solid state, resulting in a significantly smaller luminescence lifetime and quantum yield (10 μs, 1.9%), compared to the other complexes in the series. In accord with this explanation, dissolution of $Na[Yb(LF^*)_4]\cdot H_2O$ in CH_2Cl_2 restores its lifetime to 20 μs and the quantum yield to 2.4%, likely as a result of a breakup of hydrogen bonds in solution. In fact, these parameters become similar to the ones observed for the LMe^{*-} complex in solution, 20 μs and 2.6%. The smaller quantum yield for the LMe^{*-} complex in solution compared to the solid (down by 17%) results from collisional deactivations and a longer radiative lifetime (see below).

Apart from $Na[Yb(LF^*)_4]\cdot H_2O$, the lifetimes and quantum yields of the investigated complexes fall within a narrow range (±10%), suggesting that their photophysical parameters do not depend significantly on the presence of electron-withdrawing (F, Cl) or -donating (Me) groups, or a heavy atom (Br) in position 5 or 6 of the benzoxazole ring. The presence of interstitial water in the L^-, LCl^-, and LBr^- complexes does not play a significant role, except maybe for the latter (τ_{obs} and Q_L^{Yb} are down by 10%), meaning that water molecules are situated far from the metal center (no water was observed in the X-ray analysis of single crystals of these complexes). Since the coordination environment of the Yb^{III} ion is similar in all of the complexes, nonradiative deactivations and thus efficiencies of the energy transfer processes are likely to be comparable too.

These considerations can be rationalized on a more quantitative basis by considering the relevant photophysical parameters in eq 3, where Q_{Yb}^{Yb} is the intrinsic quantum yield of Yb^{III} (i.e., determined upon direct f−f excitation), η_{sens} is the efficiency with which the ligands sensitize the metal-centered luminescence, and τ_{rad} is the radiative lifetime of Yb^{III}, that is, the lifetime in absence of nonradiative deactivation:

$$Q_L^{Yb} = \eta_{sens} \times Q_{Yb}^{Yb} = \eta_{sens} \times (\tau_{obs}/\tau_{rad}) \qquad (3)$$

The radiatve lifetime of ytterbium in the complexes with LF^{*-} and LMe^{*-} in CH_2Cl_2 solution has been calculated with a modified Einstein equation (eqs 4a, 4b),[47] where c is the speed of light in centimeters per second, N_A is Avogadro's number, J and J' are the quantum numbers for the ground and excited states, respectively, $\int \varepsilon(\tilde{\nu})d\tilde{\nu}$ is the integrated spectrum of the f−f transition (Figure S20, Supporting Information); $\tilde{\nu}_m$ is the barycenter of the transition, 10 353 cm^{-1} for LF^{*-} and 10373 cm^{-1} for LMe^{*-} complexes, and n = 1.4242 for CH_2Cl_2:

$$\frac{1}{\tau_{rad}} = 2303 \times \frac{8\pi c n^2 \tilde{\nu}_m{}^2 (2J+1)}{N_A(2J'+1)} \int \varepsilon(\tilde{\nu})\, d\tilde{\nu} \qquad (4a)$$

$$\tilde{\nu}_m = \frac{\int \tilde{\nu}\cdot\varepsilon(\tilde{\nu})\, d\tilde{\nu}}{\int \varepsilon(\tilde{\nu})\, d\tilde{\nu}} \qquad (4b)$$

We find τ_{rad} = 745 μs for $Na[Yb(LF^*)_4]\cdot H_2O$ and 706 μs for $Na[Yb(LMe^*)_4]$. The ligand-to-Yb^{III} energy-transfer efficiency in solution calculated from eq 3 is therefore $\eta_{sens} \approx 1$, within experimental error. The radiative lifetimes of Yb^{III} found for these two complexes are much shorter compared to $\tau_{rad} \approx 1.2-1.3$ ms reported for Yb(diethylenetriaminepentaacetate)$^{2-}$ and Yb(dipicolinate)$_3{}^{3-}$ in aqueous solutions.[47,48] However, this comes to no surprise because radiative lifetimes of lanthanide ions are known to span large ranges,[1,47] for example, within a factor of 10 for Eu^{III}, 1−14 ms. This warns us to be very careful when estimating intrinsic quantum yields of lanthanides on the basis of "literature" radiative lifetimes (often taken as 1.2 or 2 ms for Yb^{III}).[1]

The values of τ_{rad} calculated from the absorption spectra (eqs 4a, 4b) can be double-checked by alternative calculation using eq 3 and the observed quantum yields and lifetimes. Assuming η_{sens} = 1, we get an upper limit of τ_{rad} from the ratio τ_{obs}/Q_L^{Yb} equal to 830 and 770 μs for the LF^{*-} and LMe^{*-} complexes in solution, respectively ($\eta_{sens} < 1$ would result in a smaller τ_{rad}). Therefore, τ_{rad} values calculated by two independent methods (eq 3 and eqs 4a, 4b) are similar within experimental errors.

Turning to the solid sample of $Na[Yb(LMe^*)_4]$, we obtain τ_{rad} = 630 μs from eq 3 and taking η_{sens} = 1. The change in τ_{rad} in going from solution to the solid state almost exactly matches the change expected from the difference in refractive index: considering the usually accepted value of n = 1.50 for coordination compounds in the solid state, we get a ratio $(1.50/1.4242)^2 = 1.11$ compared to $\tau_{rad}(solid)/\tau_{rad}(CH_2Cl_2) = 706/630 = 1.12$. The same calculation for $Na[Yb(LF^*)_4]\cdot H_2O$ is not valid because dissolving this complex results in the dissociation of the second-sphere water molecule, as discussed earlier.

Since the quantum yields and lifetimes of the solid samples are all in the same range, apart from $Na[Yb(LF^*)_4]\cdot H_2O$, one may hypothesize that the same highly efficient energy transfer occurs as in $Na[Yb(LMe^*)_4]$; thus assuming again η_{sens} = 1, we calculate the upper limits for radiative lifetimes to be in the range 571−635 μs (513 μs for LF^{*-}), which is consistent with the value estimated for the LMe^{*-} complex. A striking feature is the large influence of the second-sphere water molecule in $Na[Yb(LF^*)_4]\cdot H_2O$: τ_{rad} = 513 μs calculated from eq 3 is much smaller than the one expected on the basis of the change in refractive index (670 μs). To our knowledge, this is the first demonstration of a second-sphere effect on the radiative lifetime of a lanthanide ion.

(47) Werts, M. H. V.; Jukes, R. T. F.; Verhoeven, J. W. *Phys. Chem. Chem. Phys.* **2002**, *4*, 1542.

(48) Aebischer, A.; Gumy, F.; Bünzli, J.-C. G. *Phys. Chem. Chem. Phys.* **2009**, *11*, 1346.

Conclusions

The new binuclear chelates [Yb(ligand)$_2$(μ-ligand)$_2$Na] display the highest quantum yields of near-infrared luminescence reported to date for ytterbium complexes containing C−H bonds. Their unusual structure provides a binding site both for an eight-coordinate trivalent lanthanide ion and for a six-coordinate monovalent cation. An established facile synthetic modification of the ligands[31] and a variation of the monovalent cation provide opportunities for further development of these coordination compounds.

The intraligand charge-transfer state in these complexes acts as an efficient channel for the sensitization of the Yb^{III} luminescence with overall efficiency $\varepsilon \times Q_L^{Yb}$ upon excitation into its maximum at ≈450 nm being ≈300 M^{-1} cm^{-1}, that is, larger than the one reported for 8-hydroxyquinolate podates upon UV excitation.[26] Overall, these complexes compete favorably for visible light excitation of NIR luminescence of lanthanides when compared to d−f assemblies which incorporate precious metals (Pt, Ru, Os) and rely on ^{3}MLCT states as "sensitizer" levels.[49−51]

Careful analysis of the photophysical data allows us to conclude that the bright luminescence of the complexes [Yb(ligand)$_2$(μ-ligand)$_2$Na] results from a quantitative ligand-to-ytterbium energy transfer and from fast radiative deactivation of the Yb^{III} ion which competes efficiently with nonradiative pathways. The influence of the metal-ion environment, both first and second coordination spheres, on the radiative lifetime of a lanthanide ion is clearly demonstrated for the first time. These results show the importance of considering radiative decay in the design of luminescent lanthanide compounds.[47,48]

Experimental Section

General Methods, Equipment, and Chemicals Used. Elemental analyses were performed by Dr. E. Solari, Service for Elemental Analysis, Institute of Chemical and Chemical Engineering Sciences (EPFL). ^{1}H NMR spectra (presented as δ in parts per million and J in hertz) were recorded on a Bruker Avance DRX 400 MHz spectrometer. Absorption spectra were measured on a Perkin-Elmer Lambda 900 UV/vis/NIR spectrometer at room temperature in the spectral range 250−800 nm. Estimated errors are ±1 nm for λ_{max} and ±5% for ε. Luminescence emission spectra were measured on a Fluorolog FL 3-22 spectrometer from Horiba-Jobin Yvon-Spex equipped for both visible and NIR measurements and were corrected for the instrumental function. Quantum yield data were determined on the same instrument through an absolute method using a home-modified integrating sphere[48] with estimated error ± 15%. Luminescence lifetimes were measured with a previously described instrumental setup.[42,48] Spectroscopic studies were conducted under air with the samples of lanthanide complexes obtained directly from the synthesis and used without further purification in solutions in CH_2Cl_2 (Fisher Scientific, analytical reagent grade) freshly prepared before each experiment. Optical cells of 2 mm or 100 mm path length were used; solid-state sample were put into 2 mm i.d. quartz capillaries.

X-Ray Crystallography. The crystal data and structure refinement parameters are presented in Table 5. Single crystals of Na[Yb(ligand)$_4$] were grown by slow evaporation of the solution of a small sample (1−2 mg) of the complex in CH_3CN/CH_2Cl_2 for L^-, LCl^-, and LCl^{*-} or heptane/CH_2Cl_2 for L^-, LF^{*-}, and LMe^{*-}. Data collections were performed at 100(2) K using Mo K_α radiation on a Bruker APEX II CCD diffractometer, having a κ geometry goniometer. Data were reduced by means of EvalCCD[52] and then corrected for absorption.[53] Solution and refinement for all crystal structures were performed by SHELX.[54] All structures were refined using full-matrix least-squares on F^2 with all non-hydrogen atoms anisotropically defined. Hydrogen atoms were placed in calculated positions by means of the "riding" model. For complexes with LCl^{*-} and LMe^{*-}, some solvent molecules were highly disordered and then treated by means of the SQUEEZE routine of PLATON.[55] In the case of the complex with LCl^-, a rotational disorder of the benzoxazole ring of one ligand was found and treated by fitting the benzene ring to a regular hexagon and by splitting the Cl atom of the above-mentioned moiety.

Synthesis of the Ligands. The synthesis of the precursors is described in the Supporting Information. The reaction was performed under nitrogen to prevent interaction of BBr_3 with atmospheric moisture. The benzyl-protected precursor was dissolved in CH_2Cl_2 (neither dried nor degassed). This solution was cooled in an ice bath, and BBr_3 (Aldrich, 2.5 mL, 3.65 g, 15 mmol, large excess) was added dropwise, resulting in a mild exothermic reaction. The resulting red solution was warmed to room temperature and stirred for a given amount of time in the dark to give either a red solution containing a yellow precipitate or a clear red solution. The reaction mixture was cooled in an ice bath and quenched with a saturated aqueous solution of $NaHCO_3$ (dropwise addition!), resulting in an exothermic reaction accompanied by evolution of CO_2. The organic solvent was rotor-evaporated. The pH of the residual aqueous suspension was adjusted to 5−7, and it was extracted with CH_2Cl_2. The organic layer was washed with water, evaporated, and dried under a vacuum to remove the volatile organic byproduct (benzyl bromide). The solid product was redissolved in CH_2Cl_2. Either ethanol or hexane was added to this solution (their exact volumes are specified below), and CH_2Cl_2 was rotor-evaporated to give a suspension of the pure product in ethanol or hexane. It was filtered, washed with ice-cold ethanol or hexane, and dried under a vacuum. Some products are more soluble in CH_2Cl_2/ethanol mixtures than in the neat solvents. Further synthetic details are provided below.

HLMe. The reaction was performed with BnLMe (447 mg, 1.22 mmol) in CH_2Cl_2 (45 mL) for 48 h. The product was recrystallized from 10 mL of ethanol. White solid: 158 mg (0.57 mmol, 47%). Part of the product was lost during recrystallization; one may consider using hexane for recrystallization, instead of ethanol. Anal. calcd for $C_{17}H_{12}N_2O$ (MW 276.29): C, 73.90; H, 4.38; N, 10.14. Found: C, 74.48; H, 4.21; N, 10.13. ^{1}H NMR (400 MHz, $CDCl_3$): 8.46 (s, 1H, OH), 8.44 (d, J 8.4, 1H), 8.34 (d, J 8.8, 1H), 7.66 (s, 1H), 7.62−7.52 (m, 2H), 7.41 (d, J 8.4, 1H), 2.53 (s, 3H), 2H (arom.) obscured by solvent peak. ^{1}H NMR (DMSO-d_6): 10.15 (s, 1H, OH), 8.52 (d, J 8.4, 1H), 8.39 (d, J 8.4, 1H), 7.78 (d, J 8.4, 1H), 7.72 (s, 1H), 7.55 (t, J 8.0, 1H), 7.49 (d, J 8.0, 1H), 7.35 (d, J 8.4, 1H), 7.21 (d, J 7.6, 1H), 3H (CH_3) obscured by solvent peak.

HLMe*. The reaction was performed with BnLMe* (170 mg, 0.46 mmol) in CH_2Cl_2 (20 mL) for 48 h. The product was recrystallized from 20 mL of hexane. Pale yellow solid: 104 mg (0.38 mmol, 82%). Anal. calcd for $C_{17}H_{12}N_2O_2$ (MW 276.29): C, 73.90; H, 4.38; N, 10.14. Found: C, 73.53; H, 4.20; N, 9.84. ^{1}H

(49) Faulkner, S.; Natrajan, L. S.; Perry, W. S.; Sykes, D. *Dalton Trans.* **2009**, 3890.
(50) Ronson, T. K.; Lazarides, T.; Adams, H.; Pope, S. J. A.; Sykes, D.; Faulkner, S.; Coles, S. J.; Hursthouse, M. B.; Clegg, W.; Harrington, R. W.; Ward, M. D. *Chem.—Eur. J.* **2006**, *12*, 9299.
(51) Xu, H. B.; Zhang, L. Y.; Ni, J.; Chao, H. Y.; Chen, Z. N. *Inorg. Chem.* **2008**, *47*, 10744.
(52) Duisenberg, A. J. M.; Kroon-Batenburg, L. M. J.; Schreurs, A. M. M. *J. Appl. Crystallogr.* **2003**, *36*, 220.
(53) Blessing, R. *Acta Crystallogr., Sect. A* **1995**, *51*, 33.
(54) Sheldrick, G. *Acta Crystallogr., Sect. A* **2008**, *64*, 112.
(55) Spek, A. L. *PLATON. A Multipurpose Crystallographic Tool*; Utrecht University: Utrecht, The Netherlands, 2008.

Table 5. Crystal Data and Structure Refinement[a]

compound	$Na[Yb(L)_4]$	$Na[Yb(LCl)_4]$	$Na[Yb(LF^*)_4]$	$Na[Yb(LCl^*)_4]$	$Na[Yb(LMe^*)_4]$
empirical formula	$C_{64}H_{36}N_8NaO_8Yb$	$C_{64}H_{32}Cl_4N_8NaO_8Yb$	$C_{64}H_{32}F_4N_8NaO_8Yb \cdot CH_2Cl_2 \cdot H_2O$	$C_{64}H_{32}Cl_4N_8NaO_8Yb \cdot CH_3CN$	$C_{68}H_{44}N_8NaO_8Yb$
fw	1241.04	1378.81	1415.95	1419.86	1297.14
cryst syst	monoclinic	monoclinic	orthorhombic	monoclinic	monoclinic
space group	*Cc*	$P2_1/c$	$Pca2_1$	$P2_1/n$	$P2_1/n$
unit cell dimensions	$a = 20.560(4)$ Å	$a = 22.139(9)$ Å	$a = 12.8267(9)$ Å	$a = 21.762(6)$ Å	$a = 21.621(4)$ Å
	$b = 19.738(4)$ Å	$b = 19.226(6)$ Å	$b = 21.558(4)$ Å	$b = 12.2197(18)$ Å	$b = 12.220(2)$ Å
	$c = 13.130(3)$ Å	$c = 13.166(3)$ Å	$c = 20.102(5)$ Å	$c = 24.255(6)$ Å	$c = 24.913(4)$ Å
	$\alpha = 90°$	$\alpha = 90°$	$\alpha = 90°$	$\alpha = 90°$	$\alpha = 90°$
	$\beta = 107.93(3)°$	$\beta = 100.95(3)°$	$\beta = 90°$	$\beta = 101.890(17)°$	$\beta = 101.425(11)°$
	$\gamma = 90°$	$\gamma = 90°$	$\gamma = 90°$	$\gamma = 90°$	$\gamma = 90°$
vol [Å]^3	5069.2(17)	5502(3)	5558.4(17)	6312(2)	6451.6(19)
Z	4	4	4	4	4
ρ (calc) [Mg/m^3]	1.626	1.664	1.692	1.494	1.335
μ [mm^{-1}]	1.925	1.970	1.871	1.720	1.515
F(000)	2484	2740	2820	2828	2612
cryst size [mm^3]	$0.15 \times 0.15 \times 0.11$	$0.10 \times 0.09 \times 0.06$	$0.59 \times 0.20 \times 0.16$	$0.65 \times 0.21 \times 0.19$	$0.53 \times 0.13 \times 0.11$
θ range	3.51−27.50°	3.31−21.10°	3.31−27.50°	3.32−26.37°	3.30−25.00°
index ranges	$-26 \le h \le 26$	$-22 \le h \le 22$	$-16 \le h \le 16$	$-27 \le h \le 26$	$-25 \le h \le 25$
	$-25 \le k \le 25$	$-19 \le k \le 19$	$-27 \le k \le 27$	$0 \le k \le 15$	$0 \le k \le 14$
	$-17 \le l \le 17$	$-13 \le l \le 13$	$-26 \le l \le 26$	$0 \le l \le 30$	$0 \le l \le 29$
reflns collected	63380	45131	111839	12787	11309
independent reflns	11583 [R(int) = 0.0701]	5939 [R(int) = 0.1709]	12506 [R(int) = 0.0765]	12787 [R(int) = 0.0000]	11309 [R(int) = 0.0000]
completeness to θ	27.50° − 99.8%	21.10° − 99.1%	27.50° − 99.7%	26.37° − 99.1%	25.00° − 99.4%
max/min transm	1.0000/0.8480	1.0000/0.5816	1.0000/0.4822	1.0000/0.3807	1.0000/0.7903
data/restraints/params	11583/2/740	5939/1/713	12506/4/818	12787/408/802	11309/0/775
GOF on F^2	1.078	1.059	1.128	1.167	1.145
final R indices [$I > 2\sigma(I)$]	R1 = 0.0316	R1 = 0.0789	R1 = 0.0351	R1 = 0.0840	R1 = 0.0604
	wR2 = 0.0476	wR2 = 0.1804	wR2 = 0.0787	wR2 = 0.1833	wR2 = 0.1183
R indices (all data)	R1 = 0.0439	R1 = 0.1248	R1 = 0.0467	R1 = 0.1145	R1 = 0.0867
	wR2 = 0.0509	wR2 = 0.2107	wR2 = 0.0869	wR2 = 0.1977	wR2 = 0.1262
absolute structure param	0.431(5)		0.526(7)		
largest diff. peak/ hole [e/Å^3]	0.501/−0.564	4.829/−1.497	1.245/−0.986	3.468/−2.887	0.983/−1.202

[a] Data in common: Temperature, 100(2) K. Wavelength, 0.71073 Å. Refinement method, full-matrix least-squares on F^2. Absorption correction, semiempirical from equivalents.

NMR (400 MHz, CDCl3): 8.47 (s, 1H, OH), 8.43 (d, J 8.4, 1H), 8.33 (d, J 8.4, 1H), 7.75 (d, J 8.0, 1H), 7.55 (t, J 8.0, 1H), 7.51 (s, 1H), 7.40 (d, J 8.0, 1H), 2.56 (s, 3H), 2H (arom.) obscured by solvent peak. ^{1}H NMR (DMSO-d_6): 10.14 (s, 1H, OH), 8.52 (d, J 8.4, 1H), 8.38 (d, J 8.8, 1H), 7.79 (d, J 8.0, 1H), 7.72 (s, 1H), 7.55 (t, J 7.6, 1H), 7.49 (d, J 7.2, 1H), 7.31 (d, J 8.0, 1H), 7.22 (dd, J 7.2, J 0.8, 1H), 2.52 (s, 3H).

HLF. The reaction was performed with BnLF (486 mg, 1.31 mmol) in CH_2Cl_2 (15 mL) for 24 h. The product was recrystallized from 25 mL of hexane. Pale yellow solid: 248 mg (0.88 mmol, 68%). Anal. calcd for $C_{16}H_9FN_2O_2$ (MW 280.25): C, 68.57; H, 3.24; N, 10.00. Found: C, 68.34; H, 3.22; N, 9.76. ^{1}H NMR (400 MHz, $CDCl_3$): 8.48 (s, 1H), 8.43 (d, J 8.8, 1H), 8.35 (d, J 8.4, 1H), 7.65 (dd, J 8.8, J 4.0, 1H), 7.61−7.52 (m, 2H), 7.42 (d, J 8.4, 1H), 7.28 (d, J 8.0, 1H), 7.21 (td, J 9.2, J 2.4, 1H). ^{1}H NMR (DMSO-d_6): 10.18 (s, br, 1H, OH), 8.54 (d, J 8.4, 1H), 8.39 (d, J 8.4, 1H), 7.96 (dd, J 8.8, J 4.0, 1H), 7.82 (dd, J 8.4, J 2.4, 1H), 7.57 (t, J 8.0, 1H), 7.50 (d, J 7.2, 1H), 7.41 (td, J 9.6, J 2.8, 1H), 7.23 (dd, J 7.6, J 0.8, 1H).

HLF*. The reaction was performed with BnLF* (469 mg, 1.27 mmol) in CH_2Cl_2 (35 mL) for 48 h. The product was recrystallized from 15 mL of ethanol. Pale yellow solid: 191 mg (0.68 mmol, 54%). Anal. calcd for $C_{16}H_9FN_2O_2$ (MW 280.25): C, 68.57; H, 3.24; N, 10.00. Found: C, 68.82; H, 3.25; N, 10.15. ^{1}H NMR (400 MHz, $CDCl_3$): 8.42 (s, 1H, OH), 8.41 (d, J 8.4, 1H), 8.35 (d, J 8.8, 1H), 7.82 (dd, J 8.8, J 5.2, 1H), 7.57 (t, J 8.0, 1H), 7.47−7.38 (m, 2H), 7.19 (td, J 9.2, J 2.4, 1H), 1H (arom.) obscured by solvent peak. ^{1}H NMR (DMSO-d_6): 10.16 (s, br, 1H, OH), 8.53 (d, J 8.8, 1H), 8.37 (d, J 8.4, 1H), 7.96 (dd, J 8.8, J 4.8, 1H), 7.92 (dd, J 8.4, J 2.0, 1H), 7.56 (t, J 8.0, 1H), 7.50 (d, J 7.6, 1H), 7.38 (dd, J 10.0, J 2.4, 1H), 7.22 (d, J 6.8, 1H).

HLCl*. The reaction was performed with BnLCl* (621 mg, 1.61 mmol) in CH_2Cl_2 (50 mL) for 72 h. The product was recrystallized from 25 mL of ethanol. White solid: 345 mg ($C_{16}H_9ClN_2O_2$; MW 296.71). Satisfactory elemental analysis could not be obtained for this compound becuase it contained inorganic impurities. The ^{1}H NMR spectrum revealed the presence of ethanol in the sample but otherwise pointed to the absence of organic by-products. ^{1}H NMR (400 MHz, $CDCl_3$): 8.45 (s, 1H, OH), 8.42 (d, J 8.4, 1H), 8.35 (d, J 8.4, 1H), 7.79 (d, J 8.4, 1H), 7.73 (d, J 2.0, 1H), 7.58 (t, J 8.0, 1H), 7.45−7.38 (m, 2H), 7.28 (J 8.0, 1H). ^{1}H NMR (DMSO-d_6): 10.20 (s, 1H, OH), 7.54 (d, J 8.4, 1H), 8.39 (d, J 8.8, 1H), 8.13 (s, 1H), 7.95 (d, J 8.4, 1H), 7.60−7.52 (m, 2H), 7.50 (d, J 8.0, 1H), 7.22 (d, J 7.6, 1H).

Synthesis of the Complexes. The reaction was performed under air with the ligand, NaOH, and $LnCl_3 \cdot 6H_2O$ in a molar ratio of 4:4:1. The ligand was dissolved in hot THF (70−80 °C, 3 mL), followed by the addition of NaOH dissolved in water (0.75−1 mL, used as a stock solution with approximately 100 mg of NaOH per 10 mL of water) and stirring for 5 min at the same temperature. A solution of $LnCl_3 \cdot 6H_2O$ (99.9%, Aldrich) in ethanol/water (0.5/1.5 mL) was added dropwise over 5 min. A precipitate formed upon addition. The resulting suspension was stirred for 10 min at 70−80 °C, cooled to 40−50 °C, and filtered while warm. In order to remove the unreacted ligand, the solid was washed either with THF (for HL) or with THF/water (1:1, for other ligands; fresh precipitates of these complexes were soluble in THF) until filtrates were pale red. This was followed by washing with ethanol/water (1:1) and ether (until filtrates were colorless). The product was dried under a vacuum at room temperature. The complexes are air- and moisture-stable solids of orange or dark-red color. They are insoluble in water and have low solubility in organic solvents, apart from $Na[Ln(LR^*)_4]$ (R = F, Me), which are soluble in CH_2Cl_2 up to 1.3 mg/mL. Further synthetic details for Yb^{III} complexes are

provided below, while data for Lu^{III} complexes are given in the Supporting Information.

$Na[Yb(L)_4]\cdot H_2O$. Orange solid: 58 mg (0.046 mmol, 81%) from HL (60 mg, 0.229 mmol), NaOH (9.15 mg, 0.229 mmol), and $YbCl_3\cdot 6H_2O$ (22.16 mg, 0.057 mmol). Anal. calcd for $C_{64}H_{36}N_8NaO_8Yb\cdot H_2O$ (MW 1259.06): C, 61.05; H, 3.04; N, 8.90. Found: C, 61.12; H, 3.02; N, 8.48.

$Na[Yb(LF)_4]$. Dark-red solid: 63 mg (0.048 mmol, 90%) from HLF (60 mg, 0.214 mmol), NaOH (8.56 mg, 0.214 mmol), and $YbCl_3\cdot 6H_2O$ (20.74 mg, 0.0535 mmol). Anal. calcd for $C_{64}H_{32}F_4N_8NaO_8Yb$ (MW 1313.01): C, 58.54; H, 2.46; N, 8.53. Found: C, 58.46; H, 2.43; N, 8.25.

$Na[Yb(LCl)_4]\cdot(H_2O)_{0.5}$. Dark-red solid: 64 mg (0.046 mmol, 92%) from HLCl (60 mg, 0.202 mmol), NaOH (8.09 mg, 0.202 mmol), and $YbCl_3\cdot 6H_2O$ (19.59 mg, 0.0505 mmol). Anal. calcd for $C_{64}H_{32}Cl_4N_8NaO_8Yb\cdot(H_2O)_{0.5}$ (MW 1387.84): C, 55.39; H, 2.40; N, 8.07. Found: C, 55.76; H, 2.17; N, 7.75.

$Na[Yb(LBr)_4]\cdot(H_2O)_{0.5}$. Dark-red solid: 63 mg (0.040 mmol, 91%) from HLBr (60 mg, 0.176 mmol), NaOH (7.03 mg, 0.176 mmol), and $YbCl_3\cdot 6H_2O$ (17.04 mg, 0.044 mmol). Anal. calcd for $C_{64}H_{32}Br_4N_8NaO_8Yb\cdot(H_2O)_{0.5}$ (MW 1565.64): C, 49.10; H, 2.12; N, 7.16. Found: C, 49.19; H, 1.84; N, 6.90.

$Na[Yb(LMe)_4]$. Orange solid: 65 mg (0.050 mmol, 93%) from HLMe (60 mg, 0.217 mmol), NaOH (8.69 mg, 0.217 mmol), and $YbCl_3\cdot 6H_2O$ (21.04 mg, 0.054 mmol). Anal. calcd for $C_{68}H_{44}N_8NaO_8Yb$ (MW 1297.16): C, 62.96; H, 3.42; N, 8.64. Found: C, 63.27; H, 3.53; N, 8.54.

$Na[Yb(LCl^*)_4]$. Dark-red solid: 51 mg (0.037 mmol, 90%) from HLCl* (0.164 mmol), NaOH (6.57 mg, 0.164 mmol), and $YbCl_3\cdot 6H_2O$ (15.92 mg, 0.041 mmol). Anal. calcd for $C_{64}H_{32}Cl_4N_8NaO_8Yb$ (MW 1378.83): C, 55.75; H, 2.34; N, 8.13. Found: C, 56.08; H, 2.53; N, 8.12.

$Na[Yb(LF^*)_4]\cdot H_2O$. Dark-red solid: 57 mg (0.043 mmol, 81%) from HLF* (60 mg, 0.214 mmol), NaOH (8.56 mg, 0.214 mmol), and $YbCl_3\cdot 6H_2O$ (20.74 mg, 0.0535 mmol). Anal. calcd for $C_{64}H_{32}F_4N_8NaO_8Yb\cdot H_2O$ (MW 1331.03): C, 57.75; H, 2.57; N, 8.42. Found: C, 57.97; H, 2.43; N, 8.26.

$Na[Yb(LMe^*)_4]$. Orange solid: 57 mg (0.044 mmol, 81%) from HLMe* (60 mg, 0.217 mmol), NaOH (8.69 mg, 0.217 mmol), and $YbCl_3\cdot 6H_2O$ (21.04 mg, 0.054 mmol). Anal. calcd for $C_{68}H_{44}N_8NaO_8Yb$ (MW 1297.16): C, 62.96; H, 3.42; N, 8.64. Found: C, 62.84; H, 3.43; N, 8.68.

Acknowledgment. This research is supported by a grant from the Swiss National Science Foundation (Nr. 200020_119866/1).

Supporting Information Available: Synthesis of the ligand precursors and complexes, ^1H NMR spectra, absorption and luminescence spectra, CIF files of the crystal structures, CCDC 730871-730875. This material is available free of charge via the Internet at http://pubs.acs.org.